OPEN ACCESS
International Journal of Innovations in Science & Technology
RESEARCH & INNOVATION DIVISION
IJIST

Semi-Autonomous In-Pipe Inspection and Monitoring Robot for Gas Pipelines: Design, Development, and Experimental Validation

Muhammad Rafay Ali, Arshad Ali Khan, Muhammad Sudais, Muhammad Abid, Kamran Nawaz
Department of Mechanical Engineering, University of Engineering and Technology Peshawar, Peshawar, 25120, Pakistan
***Correspondence**: engrarshad@uetpeshawar.edu.pk

Citation | Ali. M. R, Khan. A. A, Sudais. M, Abid. M, Nawaz. K, "Semi-Autonomous In-Pipe Inspection and Monitoring Robot for Gas Pipelines: Design, Development, and Experimental Validation", IJIST, Vol. 8 Issue. 4 pp 1620-1638, July 2026
DOI | https://doi.org/10.33411/IJIST/1937
Received | June 10, 2026 **Revised |** July 09, 2026 **Accepted |** July 12, 2026 **Published |** July 16, 2026.

Gas pipelines form an essential component of energy infrastructure, playing a vital role in delivering natural gas safely and economically for industrial, commercial and domestic use. The networks in Pakistan are owned by Sui Northern Gas Pipelines Limited (SNGPL) and Sui Southern Gas Company (SSGC) which span thousands of kilometers or which have a total length of thousands of kilometers and therefore require periodic inspection, which is a very challenging logistical task. Traditional techniques (manual visual inspection and pipeline inspection gauges (PIGs)) are labor intensive, dangerous and often fail to detect defects during their early phase – such as micro-cracks or localized corrosion. This paper describes the design, development and experimental validation of an in-pipe inspection and monitoring robot that was designed for the 14–16-inch-diameter gas distribution pipelines. The robot incorporates two mechanisms: a pantographic mechanism is used for primary radial traction, and a telescopic mechanism is used for passive wall-contact support for different pipe diameter variations. The built-in inspection equipment includes a 5.8 GHz first-person view (FPV) camera system, a long-range communication module (LoRa SX1278, 433 MHz), a NEO-6M GPS module for defect location and a wall thickness measurement module (HC-SR04 ultrasonic sensor array). The propulsion system is powered by a set of 6 12V DC gear motors (12V60-70Rpm) which are controlled by an Arduino Mega ATmega2560 microcontroller. The prototype is made of PLA (3D-printed) and acrylic (laser cut), and its overall weight is 3.7kg, with a length is 460mm. The experimental trials successfully showed that the proposed low-cost design can achieve the following performances to enable real-time inspection of 14–16 inch gas distribution pipelines: mean traversal speed of 0.169 ± 0.002 m/s (n = 5, 95% CI: 0.167–0.171 m/s, coefficient of variation 1.2%); continuous inspection endurance of 21 min 15 s (≈215 m per run at 76 W average power draw); wall-thickness measurement repeatable within 6 mm (≤4.1% of the nominal 145 mm wall distance) at 9 out of 13 test locations; GPS defect localization being accurate to within ±2–3 m; and LoRa telemetry being accurate within sub-100 ms latency and sustained up to 1 km line-of-sight distance and 0.6 km in urban environment.

Keywords: In-pipe Inspection Robot, Gas Pipeline, Pantograph Mechanism, Ultrasonic Sensing, LoRa Communication.

Introduction:

Pipeline systems are one of the most economic and reliable methods of long-distance transportation of natural gas, crude oil and water. The history of the pipeline industry dates back to the 19th century: the first crude oil pipeline in the United States was built by Samuel Van Syckel in 1865, and was 5 miles long, replacing the use of horses for transport. Since then, pipelines have grown by leaps and bounds, connecting an estimated 2.17 million miles of pipelines worldwide. The energy sector is highly dependent on gas infrastructure in Pakistan – almost 80% of national energy production is fueled by fossil fuels, which include around 50% from gas [1]. SNGPL and SSGC together run thousands of km of high-pressure distribution pipes for various industrial, agricultural and domestic consumers all over the country [2]. The pipeline network in Pakistan has increased by 85% in the last decade alone due to the fast-increasing demands, but World Bank estimates only 21% of the population is currently connected to piped natural gas.

Despite its crucial role pipelines can be subject to a variety of degradation processes such as corrosion, erosion, mechanical stress, third party damage, and weld defects. Failure to detect can result in catastrophic consequences; explosions, environmental contamination, service disruption for an extended period of time, and loss of life. Therefore, it is necessary to conduct inspection programs systematically to identify defects at an early stage, thus avoiding the possibility of structural failure in pipelines. The need for strong inspection becomes even greater in distribution networks where pipeline sections are located below urban communities, causing post failure remediation to be significantly disruptive and expensive.

Traditional inspection approaches have a number of restrictions. The use of manual inspection can expose staff to serious occupational health risks due to the need to access confined, high pressure and toxic gas areas. Inspection gauges or "PIGs" can be used for long-distance transmission pipelines, but they are costly, require pipeline shutdown, and are unable to travel in pipelines with complex geometries, such as those with sharp bends, tee-junctions and variable diameters [3][4][5]. Such structural and economic limitations have been a big incentive for research in in-pipe inspection robotic solutions over the last 20 years.

In pipe inspection robots (IPIRs) have many attractive features: first, they remove the human operator from the dangerous environment; second, they can be used to monitor the pipeline while the pipeline is running; third, they can carry several non-destructive testing (NDT) sensors to obtain quantitative defect information [6]. Current IPIR systems range from wheeled and tracked [7][8][9][10][11] to inchworm [12], legged [13][14] and screw-driven [15] with their own compromises in terms of capabilities of traction, adaptability, power consumption and mechanical complexity. Wheeled robots with adaptive radial mechanism offer the simplest yet best compromise for distribution networks characterized by horizontal runs, moderate bends and variable diameters, which is just what SNGPL and SSGC distribution networks have.

This trend toward increased autonomy, active control and sensor fusion in IPIR platforms continues throughout the recent literature. [16] observed the taxonomy of in-pipe inspection robots had been evolving and the trend was towards hybrid passive–active adaptation mechanisms. [17] designed the Kuzhali I and Kuzhali II wheeled robots which are equipped with asymmetric and telescopic wheels, respectively, to solve the problem of motion singularity in the curved pipe sections and tested their prototypes and simulations. A single air motor was used to drive the independently adaptive wheel speeds for curved-pipe navigation in a continuously variable transmission (CVT) wheel-type robot proposed by [18]. [19] proposed an in-pipe robot with a low-cost sensor, which was designed to acquire images, and [20] developed an inertial and wheel-odometry sensor combined robot to position an in-pipe robot in underground space without GPS. Raspberry Pi and Arduino Mega have been used by [21] to construct a modular and multi-sensor crawler robot capable of autonomous navigation and multimodal defect detection, which has been demonstrated with a locomotion speed of 0.25 m/s, an obstacle-detection accuracy of 91.2%, and a battery endurance of approximately 80 min at a prototype cost of USD 1,200. Although the active/motorized adaptation mechanism [22][23], the AI-supported defect recognition and enhanced localization are increasingly cited in the literature, the systems that suit the 14–16 inch mid-pressure diameter range of distribution networks (e.g. SNGPL and SSGC), which are relevant to such applications, are still rare and have not been discussed specifically in the literature for low fabrication cost, which the present work addresses.

Although there is a wide variety of IPIR research, the majority of platforms validated are focused on smaller pipe diameters (100–200 mm) [8][9][11] found in residential or municipal gas networks in developed economies, and many of the platforms are based upon costly components or manufacturing processes which are not available in the context of developing economies. A lack of literature exists for the low-cost, modularized, and test-tuned semi-autonomous robots for 14–16 inch gas pipelines which are mostly used in the mid-pressure gas distribution system, with only isolated examples addressing substantially larger diameters [24]. This following major contributions:

In this study a dual spring-loaded adaptive locomotion mechanism (pantograph + telescopic) was developed that can achieve passive diameter adaptation in the range of 14–16 inches, integrated multi-sensor inspection system and FPV visual inspection, GPS defect localization, LoRa wireless communication and HC-SR04 ultrasonic wall-thickness measurement. Experimental assessment was carried out for the speed of locomotion, battery endurance, sensor measurement accuracy and the range of LoRa communication under realistic operating conditions. An engineering design approach was applied, suitable for the development and manufacturing in resource-limited environments.

Materials and Methods:

Design Overview:

At the beginning of the design process, it was established that the robot should be capable of passive diameter changes from 14 to 16 inches, be modular so as to make sensor upgrades easier, have a total robot mass under 5 kg for easier deployment, operate wirelessly, and be fabricated using available materials, components and fabrication services. All subsequent designs were based on these requirements.

Methodology:

The proposed in-pipe inspection robot was developed through a systematic process which started with a literature survey to find the existing design gap, then concept design and detailed design of the pantograph type adaptive mechanism. This was complemented by parallel electronic design and programming development, to integrate the sensing, locomotion and communication subsystems. During the prototype construction, the mechanical and electronic sub-assemblies were integrated and the full system was tested and validated to ensure the performance of the system for the pipe diameter range of 14 to 16 inches. . The following Figure 1 is the Methodology of the Semi-Autonomous Robot.

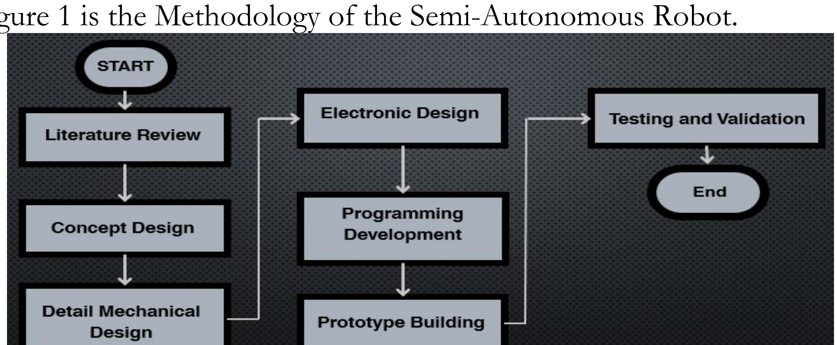

Figure 1. The Methodology of the Semi-Autonomous Robot.

Mechanical Architecture:

Overall Structure:

The architecture of the robot is based on a radial drive architecture around a central chassis containing the electronics module and two sets of drive legs, one in front and one in the back. The central chassis was designed to be hollow, so that the Arduino Mega microcontroller, motor driver boards, battery pack and communication modules could be fitted inside, and it is removable for easy access during maintenance. These components are enclosed in the electronics housing body, which is 3D-printed from PLA and which is then connected to the chassis.

The chassis has three legs on the front side and 3 on the back side, with the legs spaced 60° apart around the circumference of the chassis[25]. This even distribution of the contact force about the pipe circumference also ensures centering during traversal. There are 12 wheels of which 6 are powered by separate DC gear motors. The other six wheels roll freely and serve as passive guide wheels which minimises energy use while keeping the wheel in touch with the wall. The six HC-SR04 sensors are set up in a structured array (at about equal angular intervals) on a dedicated ultrasonic sensor tree, mounted at the front end of the robot, which gives a full circle coverage of the pipe walls. The following Figure 2 is the chasis of the robot.

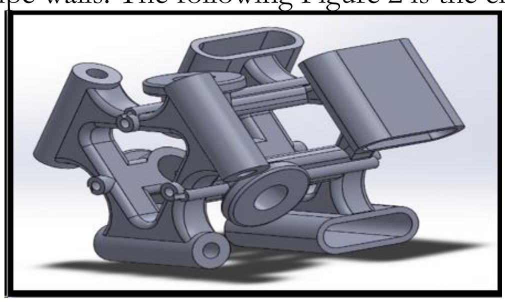

Figure 2. Chasis of Semi-Autonomous Robot.

Spring-Loaded Pantograph Mechanism:

The main adaptive mechanism is a spring-loaded pantograph (scissor linkage), made using laser cut acrylic sheet. For pantograph, the pairs of crossing linkages are joined at the center and one end is attached to the chassis hub, while the other end is attached to the wheel axle. The linkages are compressed equally, folding the pantograph and bringing the wheels closer to the centre of the chassis, as the robot approaches the narrower pipe diameter. For larger-diameter pipes, the spring stretches the linkages outward stretching the linkages outward and pushing the wheels against the pipe wall of the pipe. This mechanism offers a radial stroke of approximately 25 mm, which provides the required adaptation range for 14–16-inch-diameter pipes [26]. The following Figure 3 is spring loaded pantograph mechanism.

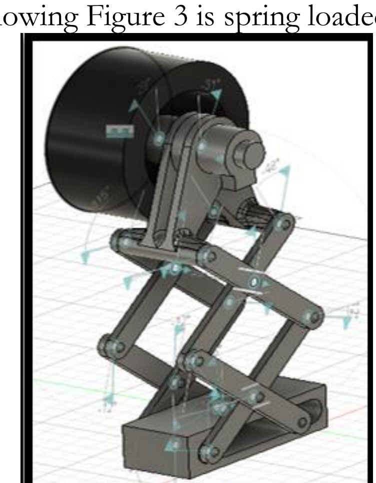

Figure 3. Spring-Loaded Pantograph Mechanism

Spring-Loaded Telescopic Mechanism:

The secondary mechanism is made up of the telescopic leg shafts in each of the six drive legs which have springs that allow them to self-retract. Each telescopic unit is made of two shafts, an outer shaft (26 mm outer diameter) and an inner shaft (same inner diameter clearance), with a compression spring in between. The spring parameters (wire diameter 2.5 mm, internal diameter 27 mm, free length 120 mm and a total number of 12 active coils) were chosen to fit in the leg assembly and were verified through compression testing [27]. It is a radial force which is applied continuously by the spring to the wheel and thus retains contact with the wheel surface regardless of the angle of the pantograph extension and complements the variable spring force profile of the pantograph. The two mechanisms combined provide normal force between all six driven wheels and the inner surface of the pipe for the entire diameter range [22]. The following Figure 4 is the Spring-loaded telescopic mechanism.

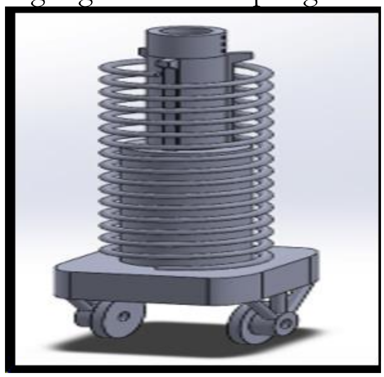

Figure 4. Spring-Loaded Telescopic Mechanism

Motor Selection:

The 12V, 60–70 RPM output speed, 3 kgcm rated stall torque brushed DC gear motors (Dc motor 12V60-70R-P4) were chosen for the drive wheels, as they are extremely lightweight and compact. Brushed DC gear motors are extremely light in weight and compact with an output speed of 60–70 RPM, rated stall torque of 3 kgcm and voltage of 12V. The torque requirement was estimated as follows: In the worst-case scenario with the robot in the vertical position, the two most loaded wheels will support the entire weight of the robot, so that each will support about $W/2 = 21.09$ N. Preload Force = $F_s \approx 20$N/wheel due to telescopic Spring. The friction force per wheel now has to be 41.09N/0.15, or 273.93N, assuming a conservative value for the kinetic coefficient of friction, $\mu = 0.15$ [27].

$F_{traction} = \mu \times F_N = 0.15 \times 41.09 = 6.16$ N

The corresponding required torque at a wheel radius of r = 42.5 mm is:

$T_{required} = F_{traction} \times r = 6.16 \times 0.0425 = 0.262$ N·m ≈ 2.67 kg·cm

In the above equation, the given variables are: a preload force F_s applied by the telescopic spring on each wheel, a net normal (wall-contact) force F_N on each wheel, μ is the assumed kinetic coefficient of friction between the tire material and the steel pipe wall, $F_{traction}$ is the required traction force on each wheel, r is the effective wheel radius, and $T_{required}$ is the required drive torque applied by each motor.

The selected motor's stall torque of 3.0 kg·cm provides a factor of safety FOS = 3.0 / 2.67 = 1.12 over the peak estimated requirement, confirming adequate torque margin for normal operations. For steeper inclinations or higher-friction conditions, a higher-torque motor variant would be advisable in future iterations. The following Figure 5 is the Motor selected.

Figure 5. DC Motor 12V 60-70 Rpm

Material Selection:

Material selection was based on five criteria: mechanical strength (tensile and compressive), thermal stability, compatibility with available manufacturing processes (3D printing and laser cutting), mass, and cost.

PLA was selected for 3D-printed structural components due to its low printing temperature (~200°C), ease of processing, acceptable tensile strength (50–70 MPa) for prototype-scale structural loads, biodegradability, and widespread availability from local suppliers. Flat structural elements requiring greater dimensional precision particularly the pantograph linkage plates were fabricated from 3 mm acrylic sheet via laser cutting, offering excellent flatness tolerance and smooth edge quality. For tire material, nitrile rubber (NBR) was selected over vulcanized rubber, polyurethane, and silicone rubber due to its excellent resistance to oils and hydrocarbons encountered in gas pipeline environments and its operational temperature range of −30°C to 120°C [28]. The following Table 1 is tire material comparison.

Table 1. Tire material comparison

Material	Hardness (Shore A)	Temperature Range (°C)	Oil Resistance	Selected
Nitrile Rubber (NBR)	40–80	−30 to 120	Excellent	Yes
Vulcanized Rubber	30–90	−50 to 80	Good	No
Polyurethane	40–95	−30 to 80	Good	No
Silicone Rubber	20–80	−60 to 230	Poor	No

Electronics and Sensor Integration:

The electronic architecture is built around the Arduino Mega (ATmega2560 microcontroller, 16 MHz clock, 256 KB Flash, 54 digital I/O pins, 16 analog inputs, 4 hardware UARTs), which coordinates all sensing, communication, and motor control operations from a central program loop. Table 2 lists the complete electronics system specifications. Table 2 lists all the electronic components and sensors used.

Table 2. Electronics and sensor system specifications

Component	Model / Specification	Function
Microcontroller	Arduino Mega ATmega2560, 16 MHz	Central control, sensor coordination, motor PWM
GPS module	NEO-6M, UART, ±2–3 m open-sky accuracy	Real-time defect location acquisition
LoRa radio	SX1278, 433 MHz, up to 15 km range (catalog)	Long-range wireless data transmission
Receiver station	custom mapping app	GPS position display on offline map
FPV camera	5 MP, wide-angle lens	Live visual inspection feed
Video transmitter	TS832, 5.8 GHz, 600 mW, NTSC/PAL	Wireless analog video link
Video receiver	RC832, 5.8 GHz, 200 mA, 75Ω	Video stream reception and display
Ultrasonic sensor	HC-SR04 × 6, range 2–400 cm	Wall thickness / distance measurement

Motor driver	L298N dual H-bridge × 3	Drive current amplification for DC motors
Battery	Li-ion 12V, 2.2 Ah (26.4 Wh)	Main power supply

Lithium Cells 2200mAh:

The robot runs on six DC gear motors, the Arduino Mega microcontroller, GPS module, LoRa transmitter, and FPV camera system all powered by ten 2200mAh lithium-ion batteries arranged in a battery pack providing the correct voltage and current to all the motors, micro, GPS, LoRa, and FPV. The type of battery used is Lithium-Ion, which has a high energy density and a stable discharge profile which results in a low overall mass of the robot and sufficient run time for a complete inspection cycle. The cells are connected in series and parallel to achieve the correct voltage of 12V, and then voltage regulated, downstream, to protect the microcontroller and sensors. The following Figure 6 is the lithium cells 2200mAh.

Figure 6. Lithium Cells 2200mAh

L298D Motor Driver:

The six DC gear motors are controlled by three L298D dual H-bridge motor driver modules, each of which can drive two motors independently. The L298D can receive low power logic signals from the Mega and control the higher current required by the motors, and is capable of sending forward/reverse/stop signals without exposing the Arduino microcontroller to motor signals. Using three separate driver boards instead of a single driver simplifies wiring and improves fault isolation, allowing each pair of motors to be fine-tuned for stable movement within the pipeline. The following Figure 7 is the Motor driver L298D.

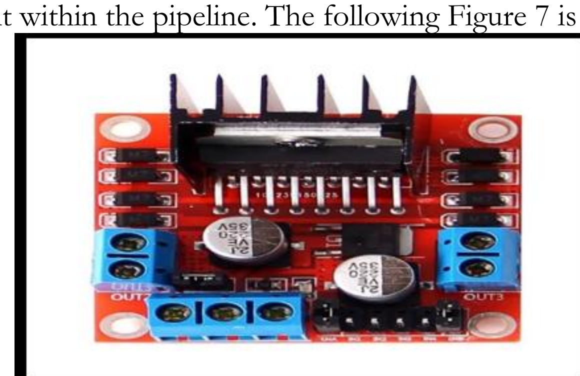

Figure 7. L298D Motor Driver

Arduino Mega:

The robot's central processing unit is an Arduino Mega, which is a microcontroller based on the ATmega2560. It has a lot of digital and analog input/output pins, enabling it to communicate with the motor drivers, the ultrasonic sensor, the GPS module, and LoRa module simultaneously without having to sacrifice input/output pins like other smaller boards. It supports multiple serial interfaces like UART, SPI, I2C and is therefore suitable to handle multiple peripherals. It gathers sensor data, performs the motor control algorithm and controls the delivery of position and inspection data to the remote station. The following Figure 8 is the Arduino used in the robot as a microcontroller.

Figure 8. Arduino Mega

Ultrasonic Sensor:

The ultrasonic sensor is used to determine the thickness of the pipe wall and detect early signs of pipe corrosion or erosion. It sends out a high-frequency pulse towards the wall, and then measures the time it takes for the echo to return, which is proportional to the thickness of the wall. The robot can be continuously sampled as it moves so that the thinning can be tracked on the pipeline as it progresses rather than just at a few individual points. The sensor is housed in a dedicated enclosure that ensures it remains in contact with the surface of the pipe and is insulated from vibration while data is recorded with GPS location to enable exact location of anomalies [29]. The following Figure 9 is the ultrasonic sensor.

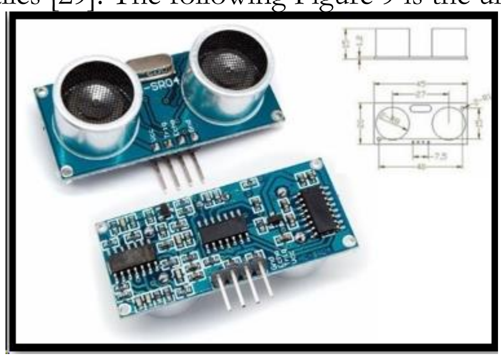

Figure 9. Ultrasonic Sensor (HC-SR04)

Transmitter, Receiver, and FPV Camera:

FPV (First-Person View) camera with a video transmitter (TS832) and receiver (RC832) offers a 'first-person' view of the pipe's interior walls. The camera is mounted in the front of the robot, and it takes continuous footage as the robot moves, which is then transmitted wirelessly over the 5.8GHz band to the receiver at the base station for instant viewing on a monitor or goggles. This provides operators with visual confirmation of the pipeline surface condition while complementing the ultrasonic thickness measurements, allowing them to avoid entering the pipeline to check for cracks, corrosion, weld defects or obstructions. The following Figure 10 is the Transmitter, Receiver and Fpv camera.

Figure10. Transmitter (TS832), Receiver (RC832) andFPV Camera

LoRa (SX1278 Module):

The LoRa SX1278 module is used to establish long-range, low-power wireless communication between the robot and remote monitoring station. Not dependent on cellular or internet infrastructure, it is well suited to gas pipeline corridors that are buried or remote, where cellular or internet connectivity is typically not available. The module sends the current GPS coordinates received by the NEO-6M receiver, as well as ultrasonic sensor readings to the base station in real time, enabling the inspector to monitor the position of the robot and the condition of the pipeline from the outside. It was selected for its point-to-point radio-link capability, providing reliable communication in enclosed environments while maintaining low power consumption with low power usage for long duration. The following Figure 11 is Lora (SX1278).

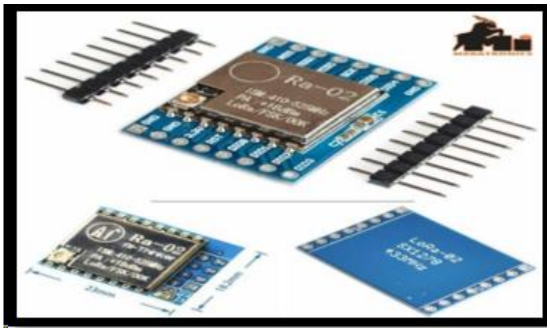

Figure 11. LoRa (SX1278 Module)

NEO-6M GPS Module:

The NEO-6M GPS module is capable of obtaining real-time geographic information of the robot, by receiving signals from multiple GPS satellites and calculating the latitude, longitude and time information. It connects with the Arduino Mega using a serial UART port, and keeps sending location data to the control system as the robot traverses the pipeline. GPS signal can be weak and unreliable underground, so the module is used in conjunction with the LoRa link to report position information to the surface, and is also used for position reporting while tracking in real time and for defect localization. This enables any deviation from normal identified by the ultrasonic sensor to be associated with a known position in the pipeline service path which can then be inspected [5]. The following Figure 12 is Neo-6M gps.

Figure 12. NEO-6M GPS Module

Control Algorithm:

The motor control is an open-loop, operator-supervised motor control scheme appropriate for the semi-autonomous, FPV-guided operating mode. The Arduino Mega runs the main program loop, which reads the six HC-SR04 sensors (with staggered trigger/echo to minimize cross-talk between adjacent sensors), decodes NMEA sentences from the NEO-6M GPS over UART, packs sensor and position data into a small frame and sends the frame over the LoRa SX1278 link, while receiving and processing PWM duty-cycle commands from the operator via UART (the operator's commands are sent from the base station, which is another Mega2560). The duty cycle (0–255) is used for open-loop wheel-speed control, but it is not closed-loop velocity feedback; the forward, reverse, stop states are set independently for each pair of motors, so that differential-style steering can be approximated by opening up the duty cycle for the front leg motors while closing the duty cycle for the rear leg motors when correcting heading inside the pipe. To prevent the Li-ion cells being over-discharged, a software interlock checks the battery voltage and stops drive output when the pack drops below a preset minimum voltage (10.5V). The robot has no closed-loop velocity or heading control, requiring the operator to make steering corrections using the live FPV feed and periodic ultrasonic/GPS telemetry, supervising the robot in a human-in-the-loop manner, as discussed further in the Future Work section regarding the transition to closed-loop autonomous control.

Prototype Fabrication:

All 3D-printed parts, such as chassis, electronics housing, motor mounts, spring retainer caps, wheel hubs, and sensor tree were 3D-printed using PLA filament with 30% infill density and 0.2 mm layer height by the company Vertex 3D as show in the figure 13 , Islamabad. 3 mm acrylic sheet was used to make pantograph linkage plates in Mardan by laser cutting. The following electronic components were obtained from local Pakistani suppliers: The HC-SR04 sensors, DC gear motors, NBR rubber tires, FPV camera, TS832 transmitter and RC832 sensor receiver were sourced from the Pakistani suppliers: Ross Electronics (Peshawar), Megatronics (Peshawar) and Electronic Solution (Lahore) respectively. While the LoRa SX1278 modules were sourced online (Karachi). The following Table 3 shows all the components used in the robot. Sizing, motor mount geometry and leg mechanism geometry were iteratively optimized through hardware prototyping and testing with the 15-inch steel pipe until the end of the product assembly. The following Figure 14 is the assembled prototype.

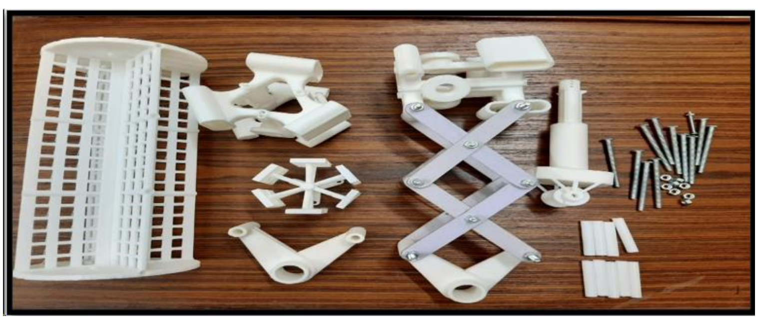

Figure 13. Body of the robot manufacture by PLA (3D printing).

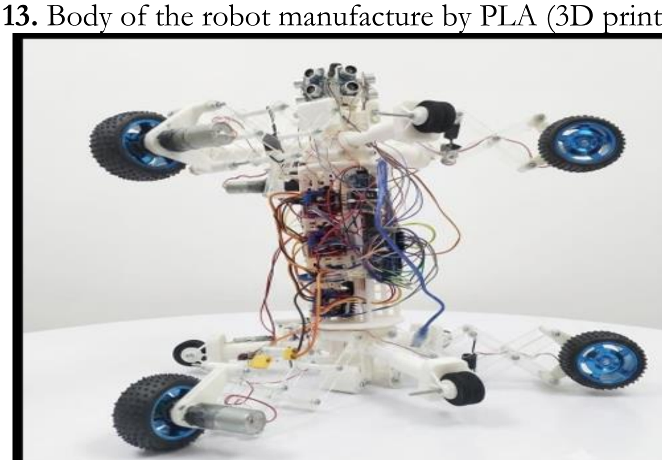

Figure 14. Complete Assembly Prototype.

Table 3. Complete robot specifications

Parameter	Specification
Robot classification	Semi-autonomous wheeled in-pipe inspection robot
Target pipe diameter	14–16 inches (356–406 mm internal)
Adaptive mechanism	Dual spring-loaded (pantograph + telescopic)
Number of driven wheels	6
Drive motors	12V, 60–70 Rpm
Microcontroller	Arduino Mega ATmega2560
GPS	NEO-6M, UART, ±2–3 m accuracy
Communication	LoRa SX1278, 433 MHz
Visual inspection	FPV 5 MP + TS832 Tx (5.8 GHz, 600 mW) + RC832 Rx
Wall sensing	HC-SR04 ultrasonic sensors
Power supply	Li-ion 12V, 2.2 Ah
Chassis / housing material	PLA (3D-printed)
Mechanism links material	Acrylic sheet (laser-cut)
Tire material	Nitrile rubber (NBR)
Motor Driver	L298D

Experimental Setup and Procedure:

The horizontally mounted 15-inch steel pipe section, 3 m long, with open ends for visual tracking of the robot's position, was used for all locomotion, sensor and communication experiments. The tests were performed in an indoor area with ambient temperature of around 22-28°C and standard humidity, where only the robot's FPV light source was used to mimic the light conditions found in a buried gas main without GPS signals. Before data collection, the HC-SR04 array was calibrated by measuring the reference distance of 50, 100, 145, 200 and 250 mm using a steel rule and a digital caliper; the mean deviation of the measured distance from the reference distance was within ±2 mm for all of them, showing good linearity of the sensors. Calibration of the NEO-6M GPS module was conducted by comparing the GPS fix data received with a known coordinate from an open sky environment for 10 minutes, prior to testing in enclosed pipes. The LoRa SX1278 link was range-tested by moving the robot-mounted transmitter and receiver away from the base-station receiver in 100 m steps for both open line-of-sight terrain and a building-obstructed (urban) environment, and observing the distance at which packets could be received without loss along with the resulting round-trip latency.

The Locomotion speed test was performed five times with the robot moving over a static 2 m portion of the test pipe, with the completion time was recorded using a stopwatch and also recorded on video for cross verification; the mean value (0.169 m/s) and the standard deviation (0.002 m/s) are calculated from these five separate tests. The battery endurance test was only performed once, with all six drive motors, FPV transmitter, GPS and six ultrasonic sensors operating continuously (all system activity), measuring from power-on until battery protection circuit shuts off supply; since this test runs a full battery charge cycle, it was not repeated in the present study and repeated-trial endurance testing is identified as a priority for future work (see Results and Future Work). At 13 different locations in the test pipe, the distance from the wall was measured using ultrasonic sensors, some of which were in areas of smooth wall, and others measured the distance from the known weld-seam locations.

Results:

The mechanical performance and locomotion performance of the inspection robot and locomotion was good for all the tested parameters of the robot. This dual-mechanism diameter adaptation system has been successfully tested in 14–16-inch diameter pipes, ensuring good wheel-wall contact and stability without requiring manual adjustment of the wheel mechanism for tilts of up to 45°. Within the 15-inch steel pipe, 5 trials were conducted that resulted in a mean speed of traversal of 0.169 m/s, and a standard deviation of only 0.002 m/s, with speed modulation in the pipe achieved and held under control at 0.05 m/s to 0.25 m/s traversal. The results of the battery endurance test with the entire system load (six drive motors, FPV camera, GPS, and six ultrasonic sensors) were 21 minutes and 15 seconds of continuous inspection flights with an average power consumption of about 76 W, representing a maximum inspection range of about 215 m per flight.

All sensor and communication systems operated well within their specifications. At 9 out of 13 locations, the six HC-SR04 ultrasonic sensors were able to measure the inner wall distance with a consistent result of 145 mm, and the difference (+3 to +6 mm) was due to surface irregularities (such as weld seams) and not considered significant, showing that the system is able to identify anomalies at levels of more than 10%. The FPV camera was able to provide good quality live video through a 5.8 GHz radio frequency channel, achieving a mean of ≥ 3.8/5.0 under four surface conditions with frame loss of 1.5m up to 12 m. For real-time defect mapping, the NEO-6M GPS module was able to provide open sky accuracy of 2–3 m. Data transmissions using the LoRa SX1278 module were reliable up to 1 km in open areas and up to 0.6 km in urban environments with a latency of less than 100 ms.

Statistical Analysis and Uncertainty:

As a repeated measure experiment, the five speeds of locomotion trials have a sample mean speed of $0.169 \pm 0.002/\sqrt{5} = 0.169 \pm 0.00089$ m/s, a standard error, and using a two-tailed t-distribution with 4 degrees of freedom ($t = 2.776$, $\alpha = 0.05$), the 95% confidence interval of the true mean traversal speed is about 0.167 m/s to 0.171 m/s, and coefficient of variation (CV = SD/mean) = 1.2%, which is low and indicates good repeatability of the locomotion mechanism under fixed test conditions. For the ultrasonic wall-distance measurements, 9 of 13 measurements (69%) agreed exactly with the reference standoff value of 145 mm with the remaining 4 measurements (31%) showing a positive deviation of 3-6 mm, or 2.1-4.1% of the nominal standoff distance, within the approximate ±2 mm measurement accuracy of the ultrasonic distance sensor plus the weld geometry deviation expected from the reference standoff value as predicted in the Discussion. No variance estimate is available for the battery endurance or FPV video-quality tests since they were performed as single tests and not repeated tests (n ≥ 3–5 tests) which are recommended for future work to provide confidence bounds for the endurance, inspection range and video mean-opinion-score (MOS) tests. The experimental performance of the robot is summarized in figure 15 for four metrics.

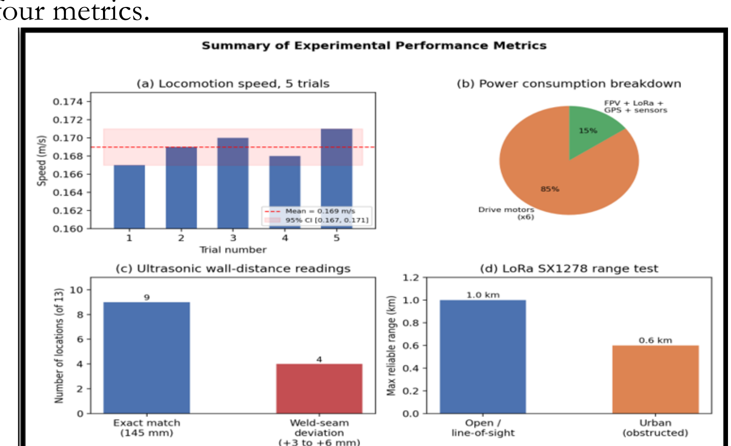

Figure 15. Summary of experimental performance metrics — (a) locomotion speed across 5 trials with 95% CI, (b) subsystem power-consumption breakdown, (c) ultrasonic wall-distance measurement consistency across 13 test locations, and (d) LoRa communication range by environment.

Discussion:

Results of the experiments validate the main design goals of the dual mechanism wheeled robot, including self-collaborating with pipeline diameters between 14 and 16 inches, stable and repeatable locomotion at inspection appropriate speed (0.169 ± 0.002 m/s), FPV video imaging for visual inspection in real-time, defect localization in real-time using GPS, and wireless data transfer without the need for internet or cellular infrastructure. There are a number of features in the design that require further elaboration.

Dual-Mechanism Adaptive System:

A fundamental trade-off between the design of passive adaptive IPIRs is how to guarantee the contact pressure between the wall and the IR elements over the whole diameter range, without any active actuators applied in the design. That is where the combined spring-loaded pantograph and telescopic mechanism come into play. The pantograph alone was determined to be inadequate since its spring force would drop as it extends to maximum radius — exactly the situation found in the larger (16") pipe where wall-contact traction is most important. This is overcome by the use of a supplementary telescopic spring which acts with an outward force which is independent of the angle of extension.

The compromise: a more complicated machine – with the dual mechanism design comes an additional 6 telescopic spring assemblies, which adds to part count and assembly time. For future designs an alternative could be to use a progressive rate spring in the pantograph linkage, stiffer at longer extensions, or a pretensioned cam linkage, which delivers a constant output of force over its stroke. These methods might yield the same diameter adaptation but in less components.

Ultrasonic Sensor:

The HC-SR04 ultrasonic sensor array offers a low-cost preliminary rough estimate of the variation of wall thickness, which is based on the air gap between the robot body and the inner wall of the pipe. There are two intrinsic factors that limit the accuracy, though. The first is that the HC-SR04 has a 15° acoustic beam angle (half-angle) which means that the measurement is an integration over a surface area and not an accurate point measurement, thereby decreasing spatial resolution for small localized defects. Second, the indirect thickness inference method (air gap measurement and subtraction from pipe measured dimensions) has positional uncertainty within the pipe cross section and dimensional variation in pipe manufacturing which leads to an accumulation of errors. The readings at weld locations which showed deviations from the nominal value of +3 to +6 mm are likely due both to the raised surface of the weld and to the effects of beam divergence.

The biggest improvement would be the replacement of the HC-SR04 array with piezoelectric contact-mode ultrasonic transducers, which offer direct measurement of wall thickness with sub-millimeter resolution through coupling and is the industry standard for UT inspection. Both contact-mode UT (coupling fluid – water or gel – plus spring loaded sensor mounting) can fit into the existing telescopic leg structure with a relatively small modification. Otherwise, EMAT sensors would be without any coupling requirement, but at a higher unit cost.

GPS Localization for Underground Pipelines:

The fact that GPS signals cannot be received underground is a natural restriction for satellite positioning and navigation – and it's not a limitation of the NEO-6M module that was chosen. In the case of pipeline deployments in urban distribution networks where pipelines are buried, a new localization strategy is needed. The most practical near term solution is to use odometry based dead reckoning with feedback from the Hall-effect encoders on the six DC gear motors [20], but the Arduino Mega has enough GPIO and UART pins to handle an encoder signal from each DC motor without making any modifications to it. If combining pipeline route GIS data, the accuracy of defect localization at the pipeline segment level could be achieved through the 200 m inspection run with an odometric error of 2–5% in wheel slip, which corresponds to a positional error of 4–10 m. Another option is to have RFID checkpoint tags at known locations along the route of the pipeline that would give periodic absolute position fixes [23] to correct for any accumulated odometric drift.

Battery Endurance and Power Optimization:

21 minutes battery endurance on a 2.2 Ah pack equates to a maximum single run inspection range of ~215 m. This is sufficient for shorter distribution segment inspections but not for longer runs of continuous inspection. Individual subsystem power profiling showed that the 6 drive motors consume around 85% of the total power and the remaining 15% is taken by the FPV system, LoRa module, GPS module, and various sensors. With minimal modification, upgrading to a 5 Ah (12V) lithium-ion pack would give approximately double the endurance – ~40 minutes – and inspection range – ~400 m. In principle a hot-swap battery design using modules is possible, where a battery pack could be removed at the pipeline entry point during the inspection run and replaced with another while the pipeline continues to operate, and this is recommended for development in the future.

Comparison with Existing Robots:

The present robot sits in a unique niche when considered against the existing robots. The MRINSPECT series [8][9] is designed for pipes of 100-200 mm diameter, and is based on active diameter adaptation using motorized radial actuators which offer greater traction control, but have higher complexity and cost. The FAMPER robot [11] is designed for tracked locomotion and is used in diameters 127–157 mm, with a good traction value and a poor value of sensor integration. Comparison of the present robot with existing and recently published (2021–2026) in-pipe inspection robots is presented in Table 4. The present design is focused on substantially larger 14–16-inch (356–406 mm) pipes, and it is passive diameter adapted and combines GPS and LoRa wireless communication into a single system — characteristics not reported in combination in the existing literature for distribution-network-scale pipelines. The prototype is significantly more cost effective than similar commercial inspection platforms.

Table 4. Comparison of the present robot with existing and recently published (2021–2026) in-pipe inspection robots

Robot (Year) [Ref.]	Pipe Diameter	Locomotion / Adaptation	Key Sensors	Reported Performance	Relative Cost
MRINSPECT series (2001–2005) [8][9]	100–200 mm	Wheeled; active motorized radial adaptation	Camera	High traction control	High
FAMPER (2010) [11]	127–157 mm	Tracked; fixed/limited adaptation	Camera	Good traction; poor sensor integration	Moderate
Kuzhali I/II (2024) [17]	Not fixed (asymmetric / telescopic wheels)	Wheeled; active + passive telescopic adaptation for curved pipes	None reported (mechanical study)	Simulated + prototype wheel forces 5–12 N	Not reported
CVT wheel robot (2024) [18]	135–185 mm	Wheeled; passive CVT + slider-crank, single-motor adaptation	Wheel encoders	Max speed 17.5 mm/s; traction 56.84 N	Moderate (air motor + CVT)
SmartCrawler (2022) [30]	Size-adaptable	Wheeled; two-phase motion control algorithm	Wireless telemetry	Size-adaptable	Moderate

	(water distribution)			operation in WDS	
Modular multi-sensor crawler (2026) [21]	Adaptive (Raspberry Pi + Arduino Mega)	Wheeled/crawler; autonomous navigation	Camera, ultrasonic, gas sensor	0.25 m/s; 91.2% obstacle detection; ~80 min endurance	~USD 1,200
Present robot (2026)	356–406 mm (14–16 in)	Wheeled; passive dual mechanism (pantograph + telescopic)	FPV, HC-SR04, GPS, LoRa	0.169 ± 0.002 m/s; 21 min / 215 m endurance	Low (local PLA/acrylic fabrication)

The present robot aims at a significantly wider pipe diameter range of 356-406 mm than recently published in-pipe inspection platforms, as seen in Figure 16. However, the MRINSPECT series [8] and [9] and the FAMPER [11] are for much smaller diameters, 100–200 mm and 127–157 mm respectively, and the CVT wheel robot [18] is in the range of 135–185 mm. This shows some literature gap with respect to low-cost and semi-autonomous robots capable for addressing larger sized mid-pressure gas distribution pipes of 14–16 inches that are studied in the present work.

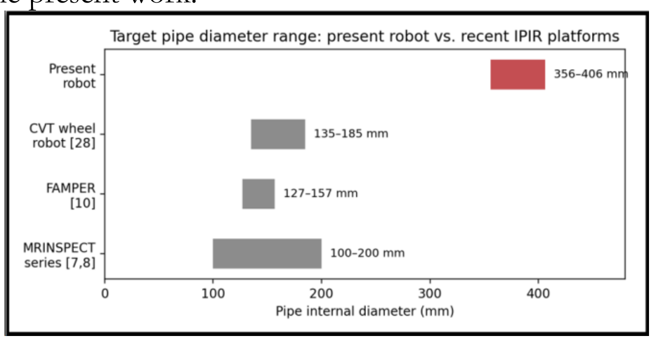

Figure 16. Target pipe diameter ranges.

Practical Implications and Industrial Significance:

In addition to technical performance, the proposed robot is also directly relevant to gas distribution utilities in resource-constrained environments. The bulk of the 14–16 inch mid-pressure distribution mains are currently only indirectly inspected (via leak survey and/or reactive maintenance after an incident has been reported), as commercial in-pipe inspection platforms costing USD 10,000-25,000 are too expensive for use at network scale within the developing-economy context. As the chassis, mechanism and housing are fabricated using locally available products of PLA and acrylic and electronic modules are used off-the-shelf, it is showcased that a functional inspection platform for this pipe class can be built and maintained using the available products and services available in Pakistan without relying on imported proprietary systems. There are three practical implications for industrial application: First, because it has low unit cost, it is viable to deploy multiple robots in parallel on multiple sections of a pipeline, instead of a single high-cost robot being shared across multiple pipelines, so it can reduce the time needed for a complete inspection cycle for a distribution segment. Second, the robot eliminates the need for the operator to work inside the pipeline, thus lowering the risk of confined space, high pressure and toxic gas exposure related to manual pipeline inspection. Thirdly, structured, geolocated defect records using GPS-tagged ultrasonic wall-thickness readings can be directly fed into a utility's predictive maintenance and regulatory compliance program, without relying on qualitative operator reports [31]. The benefits identified above, and as outlined in Future Work, could be realised at scale through the reliability, autonomy and battery endurance enhancements and by conducting tests in live or decommissioned SNGPL/SSGC pipeline sections to validate the system under real-world operating conditions.

Future Recommendation:

There are a few recognized limitations in the present work: (i) testing performed in a straight horizontal 15" diameter steel pipe, while real pipelines have bends, tee-junctions and surface contamination; (ii) the wall-thickness measurement method used is indirect, and not as accurate as the contact UT method; (iii) the current prototype is semi-autonomous (FPV-to-human loop steering) and not fully autonomous; and (iv) the battery life of 21 minutes restricts the inspection range to approximately 215 m during a single run. Future work will include: implementing 90° bends and a tee-junction by redesigning the mechanism; embedding contact-mode piezoelectric UT sensors; implementing hot-swap pack design for longer battery life; underground localization using wheel-encoder odometry; and, developing AI-assisted defect classification by combining the camera and sensor data stream. Three directions are prioritized for the second step of development. AI-based inspection: Using recent examples of image-enhancement and distortion-correction pipelines for pipe-defect imagery, a multi-sensor data stream (FPV frames, six-channel ultrasonic readings, GPS position) could be used to train a convolutional neural network to provide automated classification (corrosion, weld anomaly, mechanical damage), directly on the FPV video feed, following recent demonstrations of image-enhancement and distortion-correction pipelines for pipe-defect imagery [29][31], paired with an embedded inference platform with an embedded inference platform (e.g., a Raspberry Pi in addition to the existing Arduino Mega) to allow for near-real-time onboard classification, instead of processing recorded footage off-line. Closed-loop control: Replace the current FPV-to-human loop steering system with autonomous navigation, which would entail the use of wheel encoders or IMU-based odometry for velocity/heading feedback, and, longer term, a SLAM-based localization approach fusing odometry with intermittent GPS or RFID checkpoint fixes, consistent with approaches reported for other IPIR platforms [23][32][33], to extend the ability of the robot to navigate bends, tee-junctions and longer sections of the pipeline beyond the traditional FPV-to-human loop control system. Real world deployment: testing of the mechanism, sensors and the communication link in a real and/or decommissioned SNGPL/SSGC pipeline segment is required outside of the controlled laboratory environment to verify the mechanism's performance under real pipeline surface contamination, humidity and temperature extremes, gas-tightness/ingress protection of the electronics housing, and integration of the hot-swap battery concept and LoRaWAN gateway infrastructure to support inspection runs beyond the single-charge range demonstrated in this study.

Conclusion:

The design, fabrication and experimental verification of a semi-autonomous in-pipe inspection and monitoring robot for 14-16" gas distribution pipelines has been presented here. The work has four major contributions to the pipeline inspection robotics area. Passive (no active actuators) diameter adaptation is achieved by the use of a dual spring-loaded adaptive locomotion mechanism, which is a combination of a pantograph linkage and telescopic leg springs, providing consistent wall contact in all tested configurations between all 6 wheels. Second, an integrated multi-sensor inspection suite using FPV camera visual monitoring, GPS localization of defects, LoRa wireless communication and HC-SR04 wall thickness ultrasonic sensor provides complete real-time pipeline health monitoring without relying on a cellular or internet network. Third, experimental characterization of locomotion speed (0.169 ± 0.002 m/s), battery endurance (21 minutes / 215 m), sensor accuracy (ultrasonic deviation ≤ 6 mm) and the accuracy of FPV images (on surface $\geq 4.0/5.0$ on various surfaces) delivers the first quantitative performance data set for an IPIR platform in 14-16 inch pipeline conditions. Finally, the PLA-and-acrylic fabrication method, which leverages local manufacturing services, shows that useful inspection robotics can be developed in resource-crowded environments. The modular architecture ensures a straightforward road map for future improvements: contact-mode piezoelectric UT sensors for direct wall thickness measurement; wheel-encoder odometry for underground localization; AI-based defect classification of the jointed data stream from all sensors; wheel navigation through 90° bends; and hot-swap battery modules for longer durations. In this way, the robot is ready to be deployed in SNGPL or SSGC's energy distribution pipeline sections and will give Pakistan a reliable solution to modernize the way energy infrastructure is inspected, using a technology that can be cost-effectively automated with robots.

Acknowledgement: The authors really acknowledge the technical support of the University of Engineering and Technology, Peshawar, Pakistan

Conflict of Interest: The authors declare that there exists no conflict of interest.

Author Contributions:

Muhammad Rafay Ali: The Mechanical Design of the Robot by modeling the structure and internal layout in Solidworks, and also did the Material Selection for Durability, Weight, Corrosion Resistance and responsible for Sensor and Micro-Controller integration.

Arshad Ali Khan: Provided overall project supervision.

Muhammad Sudais: Review on in-pipe inspection technologies and the Market Survey of budget, performance, Control System design and manufacturing services.

Muhammad Abid: Responsible for the System Testing and Validation.

Kamran Nawaz: Responsible for development of Mobility Mechanism for the locomotion system.

References:

[1] "Ministry of Finance | Government of Pakistan |." Accessed: Jul. 26, 2026. [Online]. Available: https://www.finance.gov.pk/survey_archieve.html

[2] "Pakistan - Sui Northern Gas Pipelines Limited Project." Accessed: Jul. 26, 2026. [Online]. Available: https://documents.worldbank.org/en/publication/documents-reports/documentdetail/260051468284992417

[3] T. T. Nguyen, D. K. Kim, Y. W. Rho, and S. B. Kim, "Dynamic modeling and its analysis for PIG flow through curved section in natural gas pipeline," *Proc. IEEE Int. Symp. Comput. Intell. Robot. Autom. CIRA*, vol. 2001-January, pp. 492–497, 2001, doi: 10.1109/CIRA.2001.1013250.

[4] D. Mishra, K. K. Agrawal, A. Abbas, R. Srivastava, and R. S. Yadav, "PIG [Pipe Inspection Gauge]: An Artificial Dustman for Cross Country Pipelines," *Procedia Comput. Sci.*, vol. 152, pp. 333–340, Jan. 2019, doi: 10.1016/J.PROCS.2019.05.009.

[5] W. M. F. Al-Masri, M. F. Abdel-Hafez, and M. A. Jaradat, "Inertial Navigation System of Pipeline Inspection Gauge," *IEEE Trans. Control Syst. Technol.*, vol. 28, no. 2, pp. 609–616, Mar. 2020, doi: 10.1109/TCST.2018.2879628.

[6] T. R. Wanasinghe, R. G. Gosine, O. De Silva, G. K. I. Mann, L. A. James, and P. Warrian, "Unmanned aerial systems for the oil and gas industry: Overview, applications, and challenges," *IEEE Access*, vol. 8, pp. 166980–166997, 2020, doi: 10.1109/ACCESS.2020.3020593.

[7] W. Jeon, J. Park, I. Kim, Y. K. Kang, and H. Yang, "Development of high mobility in-pipe inspection robot," *2011 IEEE/SICE Int. Symp. Syst. Integr. SII 2011*, pp. 479–484, 2011, doi: 10.1109/SII.2011.6147496.

[8] S. G. Roh, S. M. Ryew, J. H. Yang, and H. R. Choi, "Actively steerable inpipe inspection robots for underground urban gas pipelines," *Proc. - IEEE Int. Conf. Robot. Autom.*, vol. 1, pp. 761–766, 2001, doi: 10.1109/ROBOT.2001.932642.

[9] S. G. Roh and H. R. Choi, "Differential-drive in-pipe robot for moving inside urban gas pipelines," *IEEE Trans. Robot.*, vol. 21, no. 1, pp. 1–17, Feb. 2005, doi:

10.1109/TRO.2004.838000.

[10] Y. S. Kwon, B. Lee, I. C. Whang, W. K. Kim, and B. J. Yi, "A flat pipeline inspection robot with two wheel chains," *Proc. - IEEE Int. Conf. Robot. Autom.*, pp. 5141–5146, 2011, doi: 10.1109/ICRA.2011.5979712.

[11] J. H. Kim, G. Sharma, and S. S. Iyengar, "FAMPER: A fully autonomous mobile robot for pipeline exploration," *Proc. IEEE Int. Conf. Ind. Technol.*, pp. 517–523, 2010, doi: 10.1109/ICIT.2010.5472748.

[12] K. Hayashi *et al.*, "Improvement of pipe holding mechanism and inchworm type flexible pipe inspection robot," *Int. J. Mech. Eng. Robot. Res.*, vol. 9, no. 6, pp. 894–899, Jun. 2020, doi: 10.18178/IJMERR.9.6.894-899.

[13] S. Savin and L. Vorochaeva, "Footstep planning for a six-legged in-pipe robot moving in spatially curved pipes," *2017 Int. Sib. Conf. Control Commun. SIBCON 2017 - Proc.*, Jul. 2017, doi: 10.1109/SIBCON.2017.7998581.

[14] S. Savin, S. Jatsun, and L. Vorochaeva, "Trajectory generation for a walking in-pipe robot moving through spatially curved pipes," *MATEC Web Conf.*, vol. 113, Jun. 2017, doi: 10.1051/MATECCONF/201711302016.

[15] T. Nishimura, A. Kakogawa, and S. Ma, "Pathway selection mechanism of a screw drive in-pipe robot in T-branches," *IEEE Int. Conf. Autom. Sci. Eng.*, pp. 612–617, 2012, doi: 10.1109/COASE.2012.6386388.

[16] A. Verma, A. Kaiwart, N. D. Dubey, F. Naseer, and S. Pradhan, "A review on various types of in-pipe inspection robot," *Mater. Today Proc.*, vol. 50, pp. 1425–1434, Jan. 2022, doi: 10.1016/J.MATPR.2021.08.335.

[17] R. Sugin Elankavi, D. Dinakaran, A. S. A. Doss, R. M. Kuppan Chetty, and M. M. Ramya, "Design of a wheeled-Type In-Pipe Inspection Robot to overcome motion singularity in curved pipes," *J. Ambient Intell. Smart Environ.*, vol. 16, no. 1, pp. 43–55, Mar. 2024, doi: 10.3233/AIS-220247;ISSUE:ISSUE:DOI.

[18] J. Park, T. Luong, and H. Moon, "Development of a Wheel-Type In-Pipe Robot Using Continuously Variable Transmission Mechanisms for Pipeline Inspection," *Biomimetics*, vol. 9, no. 2, p. 113, Feb. 2024, doi: 10.3390/BIOMIMETICS9020113/S1.

[19] K. Wu, H. Sang, Y. Xing, and Y. Lu, "Design of wireless in-pipe inspection robot for image acquisition," *Ind. Rob.*, vol. 50, no. 1, pp. 145–161, Jan. 2023, doi: 10.1108/IR-02-2022-0043.

[20] Q. Wang, M. Cai, and Z. Guo, "An enhanced positioning technique for underground pipeline robot based on inertial Sensor/Wheel odometer," *Measurement*, vol. 206, p. 112298, Jan. 2023, doi: 10.1016/J.MEASUREMENT.2022.112298.

[21] A. A. A. Eltwab and A. Sameh, "A modular, multi-sensor crawler robot for adaptive pipeline inspection: design and experimental validation," *Sci. Reports 2026 161*, vol. 16, no. 1, pp. 880-, Jan. 2026, doi: 10.1038/s41598-025-32719-y.

[22] C. Rusu and M. O. Tatar, "Adapting Mechanisms for In-Pipe Inspection Robots: A Review," *Appl. Sci. 2022, Vol. 12, Page 6191*, vol. 12, no. 12, p. 6191, Jun. 2022, doi: 10.3390/APP12126191.

[23] S. Kazeminasab, N. Sadeghi, V. Janfaza, M. Razavi, S. Ziyadidegan, and M. K. Banks, "Localization, Mapping, Navigation, and Inspection Methods in In-Pipe Robots: A Review," *IEEE Access*, vol. 9, pp. 162035–162058, 2021, doi: 10.1109/ACCESS.2021.3130233.

[24] W. Zhao, L. Zhang, and J. Kim, "Design and Analysis of Independently Adjustable Large In-Pipe Robot for Long-Distance Pipeline," *Appl. Sci. 2020, Vol. 10, Page 3637*, vol. 10, no. 10, p. 3637, May 2020, doi: 10.3390/APP10103637.

[25] S. K. P. Ankit Nayak, "Design of a New In-Pipe Inspection Robot," *Procedia Eng.*, vol. 97, pp. 2081–2091, 2014, doi: https://doi.org/10.1016/j.proeng.2014.12.451.

[26] A. S. Z. Abidin *et al.*, “Development of In-Pipe Robot D300: Cornering Mechanism,” *MATEC Web Conf.*, vol. 87, 2017, doi: 10.1051/MATECCONF/20178702029.

[27] D. Chablat, S. Venkateswaran, and F. Boyer, “Mechanical Design Optimization of a Piping Inspection Robot,” *Procedia CIRP*, vol. 70, pp. 307–312, Jan. 2018, doi: 10.1016/J.PROCIR.2018.02.015.

[28] “Different Types of Rubber: Names, Properties, and Uses.” Accessed: Jul. 26, 2026. [Online]. Available: https://flextron.org/blog/different-types-of-rubber-names-properties-uses/

[29] A. Gunatilake, L. Piyathilaka, A. Tran, V. K. Vishwanathan, K. Thiyagarajan, and S. Kodagoda, “Stereo vision combined with laser profiling for mapping of pipeline internal defects,” *IEEE Sens. J.*, vol. 21, no. 10, pp. 11926–11934, May 2021, doi: 10.1109/JSEN.2020.3040396.

[30] S. Kazeminasab and M. K. Banks, “SmartCrawler: A Size-Adaptable In-Pipe Wireless Robotic System with Two-Phase Motion Control Algorithm in Water Distribution Systems,” *Sensors 2022, Vol. 22, Page 9666*, vol. 22, no. 24, p. 9666, Dec. 2022, doi: 10.3390/S22249666.

[31] Chuka Anthony Arinze, Izionworu, Vincent Onuegbu, Daniel Isong, Cosmas Dominic Daudu, and Adedayo Adefemi, “Predictive maintenance in oil and gas facilities, leveraging ai for asset integrity management,” *Int. J. Front. Eng. Technol. Res.*, vol. 6, no. 1, pp. 016–026, Mar. 2024, doi: 10.53294/IJFETR.2024.6.1.0026.

[32] Y. S. Kwon and B. J. Yi, “Design and motion planning of a two-module collaborative indoor pipeline inspection robot,” *IEEE Trans. Robot.*, vol. 28, no. 3, pp. 681–696, 2012, doi: 10.1109/TRO.2012.2183049.

[33] S. Savin, “RRT-based Motion Planning for In-pipe Walking Robots,” *12th Int. Sci. Tech. Conf. "Dynamics Syst. Mech. Mach. Dyn. 2018*, Jul. 2018, doi: 10.1109/DYNAMICS.2018.8601473.